Theor Chem Acc (2011) 130:209–213
DOI 10.1007/s00214-011-0961-5

REGULAR ARTICLE

First-principles studies on doped graphene as anode materials in lithium-ion batteries

D. H. Wu · Y. F. Li · Z. Zhou

Received: 20 February 2011 / Accepted: 10 May 2011 / Published online: 25 May 2011

Abstract Using density functional theory computations, we investigated Li adsorption, diffusion, and desorption in pristine, B- or N-doped graphene. Compared with pristine graphene, B-doping significantly enhances Li adsorption, whereas Li adsorption is slightly weakened on N-doped graphene, which should be attributed to the different electronic structures due to doping. Li diffusion on various graphene systems was also computed through nudged elastic band method, and the results revealed that Li diffusion on N-doped graphene is faster than on pristine and B-doped graphene. Moreover, for Li desorption from the graphene substrate, N-doped graphene showed the lowest desorption barrier. Our results are in agreement with recent experimental reports and also demonstrate that N-doped graphene is a promising anode material with high-rate charge/discharge ability for Li-ion batteries.

Keywords Graphene · Lithium–ion batteries · Doping · N-doped graphene · Anode materials

1 Introduction

Lithium–ion batteries (LIBs) have been widely used in portable electronic devices, such as cellular phones and laptop computers, and are expected to provide energy for electric vehicles and hybrid electric vehicles. Graphite-based materials are usually used in anodes for commercial LIBs nowadays. However, the theoretical specific capacity of graphite is only 372 mAh/g and cannot meet the ever-growing need of the current society. Carbon nanotubes have ever been explored as LIB anode materials [1–7] and exhibited excellent lithium storage capability. Both graphite and carbon nanotubes are allotropic forms of carbon.

A new allotropic form of carbon, graphene, is a two-dimensional (2D) sheet of sp^2-hybridized carbon with unusual properties [8]. In 2004, graphene was experimentally realized in Geim's group [9]. Since then, lots of studies have focused on this new marvelous material [10–13] and exploited its potential applications, including LIB materials [14–18]. It has been reported that the specific capacity of graphene was 945 mAh/g in the first cycle and maintained 460 mAh/g after 100 cycles [18], mainly because graphene can adsorb lithium on both sides. At the same time, the single layer would be very smooth for lithium to diffuse since the space for lithium is much larger than the interlayer space in graphite. Recently, theoretical studies have also been performed on graphene as LIB anode materials [19–22]. Doped graphene has also been synthesized experimentally; by chemical vapor deposition (CVD) method, N-doped graphene was synthesized [23], and arc discharge method was applied to synthesize both B- and N-doped graphene [24]. More recently, some new methods have been employed to synthesize N-doped graphene [25, 26]. N-doped graphene was examined as LIB anode material experimentally and exhibited some advantages [27].

B- and N-doping effects in graphite were examined both experimentally and theoretically [28–32], and computational investigation was also performed on doped carbon

Dedicated to Professor Shigeru Nagase on the occasion of his 65th birthday and published as part of the Nagase Festschrift Issue.

D. H. Wu · Y. F. Li · Z. Zhou (✉)
Institute of New Energy Material Chemistry,
College of Chemistry, Key Laboratory of Advanced
Energy Materials Chemistry (Ministry of Education),
Nankai University, Tianjin 300071, China
e-mail: zhouzhen@nankai.edu.cn

nanotubes as LIB anode materials [33–37]. How do B- and N-doping affect the Li storage in graphene? In this work, we performed density functional theory (DFT) computations to compare the Li adsorption, diffusion, and desorption in pristine and B- or N-doped graphene.

2 Computational method

All first-principles computations were performed by using DMol^3 package [38, 39], and the generalized gradient approximation (GGA) and PW91 functional [40] were employed. A double numerical basis set was chosen, and the orbital cutoff was 5.1 Å. Self-consistent field calculations were conducted with convergence criteria of 10^{-5} a.u for the total energy. A $4 \times 4 \times 1$ k-point was used to sample the 2D Brillouin zone, and the spin was unrestricted. Nudged elastic band (NEB) method in the DMol^3 package was employed for the computations of transition state search and minimum energy path (MEP).

In all computations, a $4 \times 4 \times 1$ supercell including 32 atoms was used to model 2D graphene. For adsorption energy calculation, only one atom was substituted in the doped structure, corresponding to the doping concentration of 3.1 at%. For the computations of diffusion process and electronic structure, we still adopted the $4 \times 4 \times 1$ supercell, but instead of only one doping atom, four atoms were substituted in the supercell, corresponding to the doping concentration of 12.5 at%. These two models are illustrated in Fig. 1. The above doping concentrations of N are comparable to the values ($\sim$2% [41] and $\sim$9% [27]) in the recent experimental reports.

The adsorption energy, E_{ad}, of lithium, is defined as below:

$$E_{ad} = E_{Li} - E_{Graphene} - E_{Graphene-Li}$$

In the equation, E_{Li}, $E_{Graphene,}$, and $E_{Graphene\text{-}Li}$ represent the total energy of lithium atom, graphene, and graphene-Li complex, respectively.

3 Results and discussion

Three possible Li adsorption sites are defined as Atom, Bond, and Hollow site (Fig. 1), indicating that Li atom is attached above the atom, the middle of the bond, and the center of the six-membered ring (6MR), respectively. Though previous study indicates that the most stable site for lithium is the hollow one in graphene nanoribbons [20], we still considered all the three adsorption sites for better understanding the adsorption behaviors. However, when lithium was initially set above the atom or the bond site, it would migrate to the hollow site after geometry optimization, which indicates that the hollow site is indeed the most preferable adsorption position for Li. The lithium adsorption energies are summarized in Table 1 for three kinds of graphene. The Li adsorption energy is the largest in B-doped graphene and the smallest in N-doped graphene.

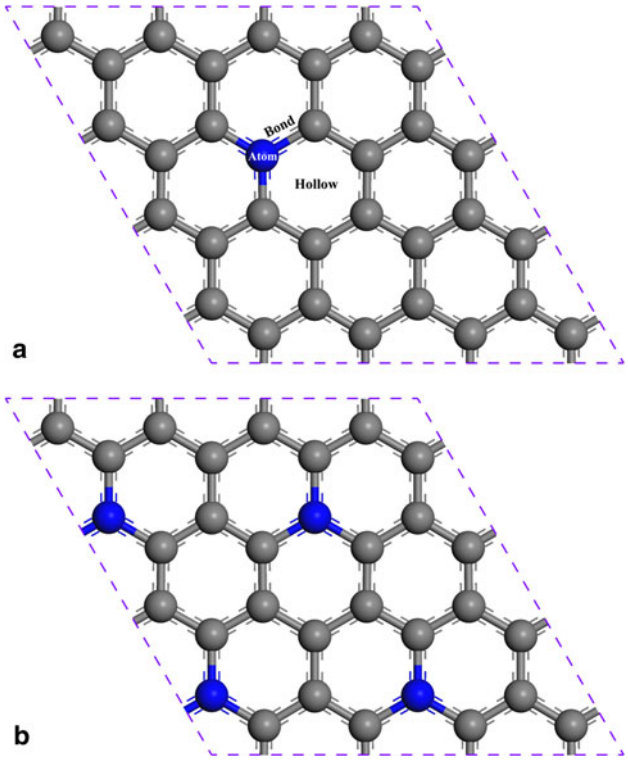

Fig. 1 Supercells for the computations of lithium adsorption (**a**) and diffusion (**b**). *Grey* and *blue* atoms represent carbon and doped (B or N) atoms, respectively

Table 1 Adsorption energies (E_{ad}'s) of Li in pristine, B- and N-doped graphene

	E_{ad} (eV)
B-doped graphene	2.71
Pristine graphene	1.36
N-doped graphene	0.88

Next, in order to get further insight into the different adsorption situations of Li in various systems, we computed and analyzed the electronic structures. Figure 2 shows the density of states (DOS) for three graphene systems. Obviously, pristine graphene is a semimetal, in agreement with the previous report [11]. Nitrogen doping lifts its Fermi level into the conduction band. On the contrary, boron doping lowers the Fermi level into the valance band. Therefore, boron and nitrogen doping will not obstruct the good conductivity of graphene, in accordance with previous reports [42, 43]. Also, the partial DOS

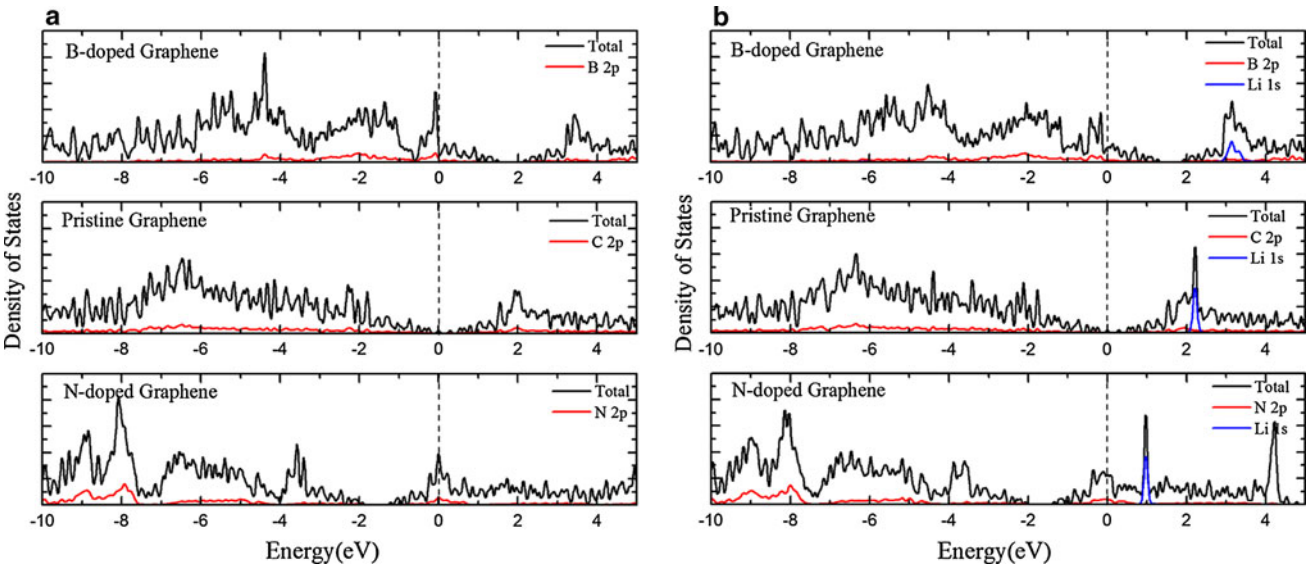

Fig. 2 DOS of various graphene systems before (**a**) and after (**b**) Li adsorption

(PDOS) for Li atom in all the three Li-adsorbed systems are also compared; Li contributes only to the conduction band, which indicates that Li is fully ionized and the interaction between Li and graphene is mainly Coulomb interaction. Li is an electron donor under this situation, while B-doped graphene is an electron-deficient system, and there are many empty states above the valance band; therefore, Li atom tends to lose its electrons to the electron-deficient system more preferable. On the contrary, N-doped graphene is an electron-rich system, and there are many occupied states below the conduction band; therefore, such system does not tend to accept electrons from Li atom, leading to lower adsorption energy.

Boron and nitrogen doping can change the Li adsorption energies; however, it is still not clear how boron and N-doping affect the Li diffusion on graphene. For comparing the Li diffusion behaviors on pristine and doped graphene, as shown in Fig. 3, we define the original site O and six possible sites for Li diffusion at next step, sites A, B, C, D, E, and F. For pristine graphene, all the six sites are identical. Using NEB method, we computed the diffusion barrier and MEP from O to all the possible sites. The results are summarized in Fig. 4.

We can see from Fig. 4 that all the diffusion barriers are very low in the three graphene systems. In diffusion path O–A and O–B, the diffusion barriers of B-doped graphene is a little lower than those in pristine graphene and N-doped graphene; however, in the other four diffusion paths, the diffusion barrier of B-doped graphene is the highest, indicating that there is strong attractive interaction between Li and B, and then it becomes difficult for Li to migrate away from B atom and it is relatively easy to migrate across B atom. In nitrogen-doped graphene, all diffusion barriers are

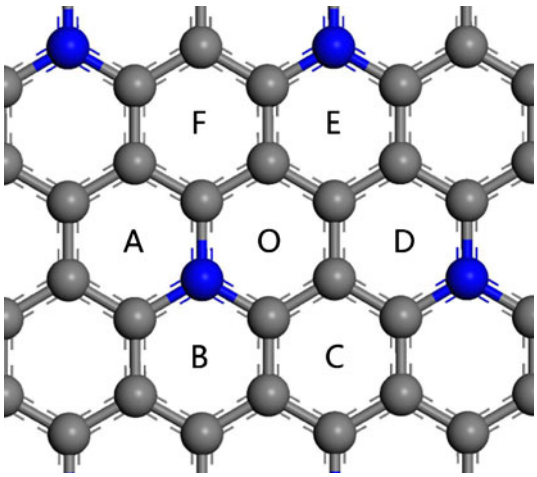

Fig. 3 Six possible sites for Li diffusion. In pristine graphene, all the six sites are identical. In doped graphene, lithium adsorption energies at O, A, B, D, and E sites are equal

lower than those of pristine graphene, while only in the diffusion paths O–A and O–B, the diffusion barriers are a little higher than those in B-doped graphene, which indicates that there is repulsive interaction between Li and N; therefore, Li tends to migrate away from N atom. In general, N-doped graphene shows better diffusion performances than pristine and B-doped graphene.

Delithiation process was also examined by computing MEP of moving Li from the most stable adsorption site to a site 2.5 Å far away above the original one; the results are shown in Fig. 5. From Fig. 5, we can easily conclude that the enhanced adsorption in B-doped graphene would surely bring a difficult desorption for Li, and Li atoms may be trapped at the electron-deficient B-doped graphene.

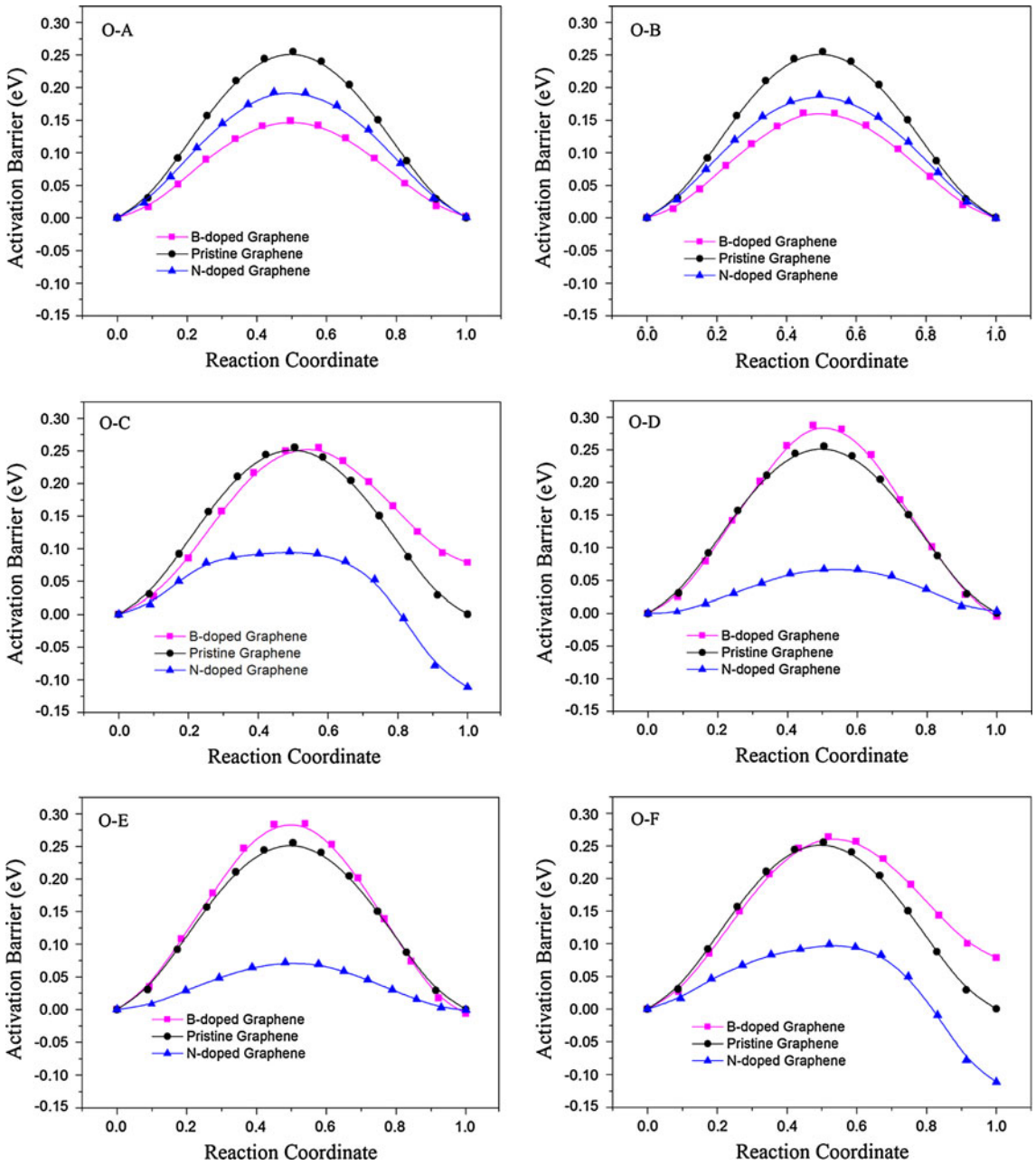

Fig. 4 Energy profile along the Li migration path O–A, O–B, O–C, O–D, O–E, and O–F

Accordingly, Li intercalation/deintercalation should occur at high potentials and would not be fluent in practical LIB anodes. In contrast, the lower lithium adsorption and desorption energies in N-doped graphene would get delithiation process more easily.

In general, N-doped graphene provides low Li intercalation/deintercalation potential and high diffusion ability and seems promising anode materials for Li-ion batteries. Recently, Reddy et al. [27] have also found in their experiments that N-doped graphene showed very low insertion potential and also excellent high-rate charge/discharge performances. Though they attributed the improvement to the intimate contact between the electrode and current collector, our computational results demonstrate that low potential and excellent high-rate performance are also intrinsic characteristics of N-doped graphene. Low diffusion and desorption barriers would lead to very high Li diffusion rates. Extensive experiments are welcome to further exploit this promising anode material for Li-ion batteries.

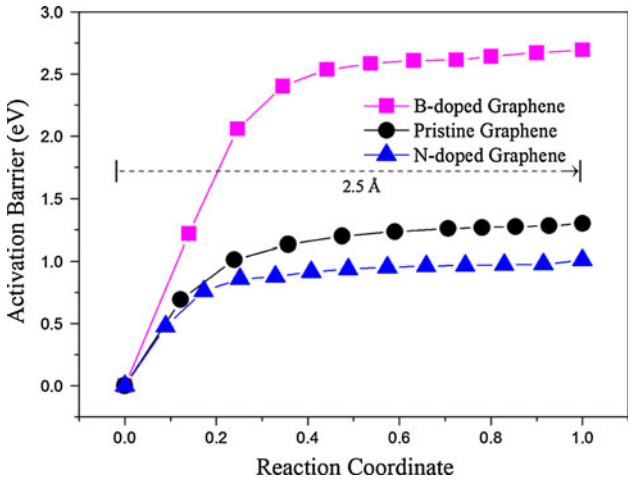

Fig. 5 Energy change during delithiation process; the activation barrier is virtually equal to lithium adsorption energy

4 Conclusion

In summary, we performed detailed density functional theory computations to investigate Li adsorption, diffusion, and desorption in pristine and B or N-doped graphene. Boron doping enhances lithium adsorption, while nitrogen doping weakens lithium adsorption. For Li diffusion, N-doped graphene shows lower diffusion and desorption barrier, indicating that N-doped graphene may present high-rate charge/discharge performances. We have disclosed some advantages in N-doped graphene as anode materials for Li-ion batteries. Since it is much more complicated in practical Li-ion batteries, further experimental investigations are needed to understand the performances, and to confirm the great potentials of N-doped graphene in Li-ion batteries.

Acknowledgments This work was supported by National Innovation Experiment Program for University Students (101005531) in China.

References

1. Zhao JJ, Buldum A, Han J, Lu JP (2000) Phys Rev Lett 85:1706–1709
2. Meunier V, Kephart J, Roland C, Bernholc J (2002) Phys Rev Lett 88:075506
3. Gao B, Bower C, Lorentzen JD, Fleming L, Kleinhammes A, Tang XP, McNeil LE, Wu Y, Zhou O (2000) Chem Phys Lett 327:69–75
4. Frackowiak E, Béguin F (2002) Carbon 40:1775–1787
5. Landi BJ, Ganter MJ, Cress CD, DiLeo RA, Raffaelle RP (2009) Energy Environ Sci 2:638–654
6. Liu Y, Yukawa H, Morinaga M (2003) Adv Quantum Chem 42:315–330
7. Song B, Yang JW, Zhao JJ, Fang HP (2011) Energy Environ Sci 4:1379–1384
8. Geim AK (2009) Science 324:1530–1534
9. Novoselov KS, Geim AK, Morozov SV, Jiang D, Zhang Y, Dubonos SV, Grigorieva IV, Firsov AA (2004) Science 306:666–669
10. Allen MJ, Tung VC, Kaner RB (2009) Chem Rev 110:132–145
11. Geim AK, Novoselov KS (2007) Nat Mater 6:183–191
12. Niyogi S, Bekyarova E, Itkis M, McWilliams J, Hamon M, Haddon R (2006) J Am Chem Soc 128:7720–7721
13. Rao CNR, Sood AK, Voggu R, Subrahmanyam KS (2010) J Phys Chem Lett 1:572–580
14. Liang MH, Zhi LJ (2009) J Mater Chem 19:5871–5878
15. Guo P, Song HH, Chen XH (2009) Electrochem Commun 11:1320–1324
16. Lian P, Zhu X, Liang S, Li Z, Yang W, Wang H (2010) Electrochim Acta 55:3909–3914
17. Pan DY, Wang S, Zhao B, Wu MH, Zhang HJ, Wang Y, Jiao Z (2009) Chem Mater 21:3136–3142
18. Wang GX, Shen XP, Yao J, Park J (2009) Carbon 47:2049–2053
19. Uthaisar C, Barone V (2010) Nano Lett 10:2838–2842
20. Uthaisar C, Barone V, Peralta JE (2009) J Appl Phys 106:113715
21. Khantha M, Cordero NA, Molina LM, Alonso JA, Girifalco LA (2004) Phys Rev B 70:125422
22. Wang XL, Zeng Z, Ahn H, Wang GX (2009) Appl Phys Lett 95:183103
23. Wei D, Liu Y, Wang Y, Zhang H, Huang L, Yu G (2009) Nano Lett 9:1752–1758
24. Panchakarla LS, Subrahmanyam KS, Saha SK, Govindaraj A, Krishnamurthy HR, Waghmare UV, Rao CNR (2009) Adv Mater 21:4726–4730
25. Deng DH, Pan XL, Yu L, Cui Y, Jiang YP, Qi J, Li W-X, Fu Q, Ma XC, Xue QK, Sun GQ, Bao XH (2011) Chem Mater 23:1188–1193
26. Zhang CH, Fu L, Liu N, Liu MH, Wang YY, Liu ZF (2011) Adv Mater 23:1020–1024
27. Reddy ALM, Srivastava A, Gowda SR, Gullapalli H, Dubey M, Ajayan PM (2010) ACS Nano 4:6337–6342
28. Way BM, Dahn JR (1994) J Electrochem Soc 141:907–912
29. Weydanz WJ, Way BM, Vanbuuren T, Dahn JR (1994) J Electrochem Soc 141:900–906
30. Morita M, Hanada T, Tsutsumi H, Matsuda Y, Kawaguchi M (1992) J Electrochem Soc 139:1227–1230
31. Kurita N (2000) Carbon 38:65–75
32. Endo M, Hayashi T, Hong S-H, Enoki T, Dresselhaus MS (2001) J Appl Phys 90:5670–5674
33. Zhou Z, Gao X, Yan J, Song D, Morinaga M (2004) J Phys Chem B 108:9023–9026
34. Zhou Z, Gao X, Yan J, Song D, Morinaga M (2004) Carbon 42:2677–2682
35. Zhou Z, Zhao J, Gao X, Chen Z, Yan J, Schleyer PVR, Morinaga M (2005) Chem Mater 17:992–1000
36. Zhao JJ, Wen B, Zhou Z, Wang JL, Chen ZF, Schleyer PVR (2005) Chem Phys Lett 415:323–326
37. Li YF, Zhou Z, Wang LB (2008) J Chem Phys 129:104703
38. Delley B (1990) J Chem Phys 92:508–517
39. Delley B (2000) J Chem Phys 113:7756–7764
40. Perdew JP, Wang Y (1992) Phys Rev B 46:12947–12954
41. Wang HB, Zhang CJ, Liu ZH, Wang L, Han PX, Xu HX, Zhang KJ, Dong SM, Yao JH, Cui GL (2011) J Mater Chem 21:5430–5434
42. Lherbier A, Blase X, Niquet Y-M, Triozon F, Roche S (2008) Phys Rev Lett 101:036808
43. Li YF, Zhou Z, Shen PW, Chen ZF (2009) ACS Nano 3:1952–1958